ON THE ONSET OF INSTABILITIES IN A BÉNARD-MARANGONI PROBLEM IN AN ANNULAR DOMAIN WITH TEMPERATURE GRADIENT

by

Sergio HOYAS[1*], Andrea IANIRO[2], María J. PEREZ-QUILES[1], and Pablo FAJARDO[2]

[1] Instituto Universitario de Matemática Pura y Aplicada, Universitat Politécnica de Valéncia.

[2] Aerospace Engineering Group, Universidad Carlos III de Madrid.

Original scientific paper
DOI: ???

This manuscript addresses the linear stability analysis of a thermoconvective problem in an annular domain. The flow is heated from below, with a linear decreasing horizontal temperature profile from the inner to the outer wall. The top surface of the domain is open to the atmosphere and the two lateral walls are adiabatic. The effects of several parameters in the flow are evaluated. Three different values for the ratio of the momentum diffusivity and thermal diffusivity are considered: relatively low Prandtl number (Pr = 1), intermediate Prandtl number (Pr = 5) and high Prandtl number (ideally $Pr \to \infty$, namely Pr = 50). The thermal boundary condition on the top surface is changed by imposing different values of the Biot number, Bi. The influence of the aspect ratio (Γ) is assessed for through by studying several aspect ratios, Γ. The study has been performed for two values of the Bond number (namely Bo = 5 and 50), estimating the perturbation given by thermocapillarity effects on buoyancy effects. Different kind of competing solutions appear on localized zones of the Γ-Bi plane. The boundaries of these zones are made up of co-dimension two points. Co-dimension two points are found to be function of Bond number, Marangoni number and boundary condition but to be independent on the Prandtl number.

Key words: *Marangoni problem Thermocapillary convection Linear stability Buoyancy Effects*

Introduction

It is well known that two different effects are responsible of the thermoconvective instabilities in fluid layers: gravity and capillarity forces. The problem in which both effects are considered, known as Bénard-Marangoni (BM) convection, has become a classical problem in fluid mechanics [1]. In the classical BM problem, heat is uniformly applied from the bottom wall and the solution becomes unstable for increasing temperature gradients. A more general problem includes the effect of horizontal temperature gradients resulting in new thermoconvective instabilities. Broadly speaking, the problem described could be treated as

* Corresponding author; e-mail: serhocal@mot.upv.es

shallow water problem, see [2], but the objective of the current study is different since it relies on the analysis of the onset of instabilities.

The practical importance of the BM problem is nowadays widely recognized since it appears in a wide variety of processes such as the flow inside distillation columns, silicon crystal growth, film coating processes or the drying process by evaporation [3]. Mercier et al. [4] showed that the transition to a stationary convective mode can take place even if an adiabatic boundary condition is replaced with a Newton's law.

These instabilities have been analyzed considering either rectangular domains containing the flow [5, 6], either annular geometries [7], or infinite liquid films [8]. Literature includes some attempts to develop a theoretical framework for these problems, as presented in [9] and references therein, but for the moment it seems that more effort is required to develop more powerful numerical and mathematical tools to fully understand the process.

The following set of dimensionless numbers has been usually employed to characterize the different effects steering the behavior of the flow:

1. Aspect ratio, $\Gamma=\delta/d$. It is the geometrical parameter that characterizes the domain.

2. Prandtl number, Pr: the ratio of momentum diffusivity (kinematic viscosity) to thermal diffusivity. In this manuscript several Pr values are considered, ranging from unity to very high value (~50) : $\mathrm{Pr}=\nu/\kappa$.

3. Marangoni number, Ma. It accounts for surface tension effects: $\mathrm{Ma}=\gamma_T \Delta T d/\rho\kappa\nu$

4. Rayleigh number, Ra. It is representative of the importance of the buoyancy effects: $\mathrm{Ra}=g\alpha\Delta T d^3/\kappa\nu$.

5. The two previously defined numbers are combined as the Bond number, Bo, which is the ratio of Rayleigh to Marangoni numbers, and thus represents the buoyancy against surface tension effects: $\mathrm{Bo}=\mathrm{Ra}/\mathrm{Ma}=\rho g\alpha d^2/\gamma_T$.

6. Biot number, Bi, describes the heat transfer at the upper boundary condition between the fluid and the atmosphere. Values inside the range [0.2-3.2] have been considered in this work.

In the previous definitions, δ and d are the characteristic lengths of the domain that will be defined in the following section; γ_T stands for the rate of change of surface tension with temperature; ΔT is the temperature increment at the lower boundary with respect to the ambient temperature; ρ, κ, α and ν are the density, the thermal diffusivity, the thermal expansion coefficient and the kinematic viscosity of the fluid, respectively; and g is the acceleration due to gravity. It is convenient to remark that the Bond number used in the present work is the thermal Bond number defined as the ratio between thermogravitational effects and thermocapillarity effects, which should not be confused with the Bond number commonly used in interfacial systems. Since the objective of present study is to analyze phenomena in which the buoyancy is dominant, the Bond number range of interest includes values greater than one. The importance of heat-related parameters on the development of instabilities was analyzed in [10, 11]. More recently, the problem was also studied in annular geometries [12, 13] but neglecting the effect of heat transfer from the top surface and considering conduction through the lateral walls of the cylinder. Literature includes also works dealing with localized heating [14], or containers heated by a non-uniform flux [3]. Hoyas et al. [15] analyzed the effect of the Biot number on the different bifurcations for the case of $\mathrm{Pr}=\infty$. The computational method was validated by comparing the results obtained

with the experimental results by Garnier et al. [16]. The computational method was modified to deal with Prandtl numbers close to unity as shown in [17]. In [18], the authors investigated the existence of co-dimension three bifurcations that are the points where co-dimensions two curves intersect on the Prandtl-Biot plane, and a new kind of instability was predicted. Those latter works dealt with the influence of Biot number on the flow solutions. Also, the interest in understanding the influence of gravitational effects in thermo-convective phenomena has been rapidly growing [19, 20, 21]. Very recently the authors have studied the influence of the domains geometry on the onset of instabilities [22].

Depending on the symmetries of the growing perturbation, several bifurcations may appear. Up to six different competing solutions for the different wave numbers have been found, namely:

- stationary rolls (SR), similar to the ones of the basic state [23]
- hydrothermal wave of the first kind or oblique traveling waves (HWI) [23]
- longitudinal rolls (LR) [15]
- standing hydrothermal wave of second class or flower-like wave (HWII) [16, 24]
- two new kinds of hydrothermal waves recently reported by Hoyas et al. [22] for low values of Γ.

The present work is devoted to analyze the effect of the gravitational and capillarity forces of the onset of flow instabilities by means of flow computations. It is worth to keep in mind that an adequate understanding of the way in which this instabilities are developed will create new possibilities of controlling them. In this work the effect of 3 different Prandtl numbers, ranging from a viscosity dominated problem ($Pr\approx\infty$, namely equal to 50) to problems in which the nonlinear flow effects are important (Pr=1). An intermediate value of the Prandtl number representative of the conditions of water at ambient conditions (Pr=5) is also considered. Additionally, the work is performed for two different Bond number conditions Bo = 50 which means negligible thermocapillarity effects and Bo = 5 to evaluate the influence of the surface tension in perturbing the computed instabilities.

The paper is structured as follows: in the second section the mathematical model of the flow behavior is proposed and in the third one the computational method implemented to obtain the solution is described. Then, in the fourth section the results are discussed. Finally, in the last section the main conclusions are presented.

Model description and formulation

The physical domain considered in this work consists of a horizontal fluid layer of depth d (z coordinate) contained in the annular ring limited by two concentric cylinders of radii a and $a+\delta$ (r coordinate). A sketch of the domain is presented in Fig. 1. The diameters of the two cylinders are chosen so that the bigger is the double of the smaller one, i.e., $a=\delta$). The geometry of the fluid domain is characterized by the aspect ratio, Γ.

The bottom surface is considered to be rigid and is heated with a linear decreasing (along the radius) temperature gradient with a temperature difference T_G = 2 K, which is kept constant throughout this study. The reference temperature used in the definition of the Rayleigh and Marangoni numbers is the mean temperature difference between the bottom plate and the atmosphere, ΔT. The top surface is open to the atmosphere and the heat transfer to the atmosphere is expressed in terms of the Biot number (as shown in Table 1). The two lateral walls of the cylinder are considered as adiabatic.

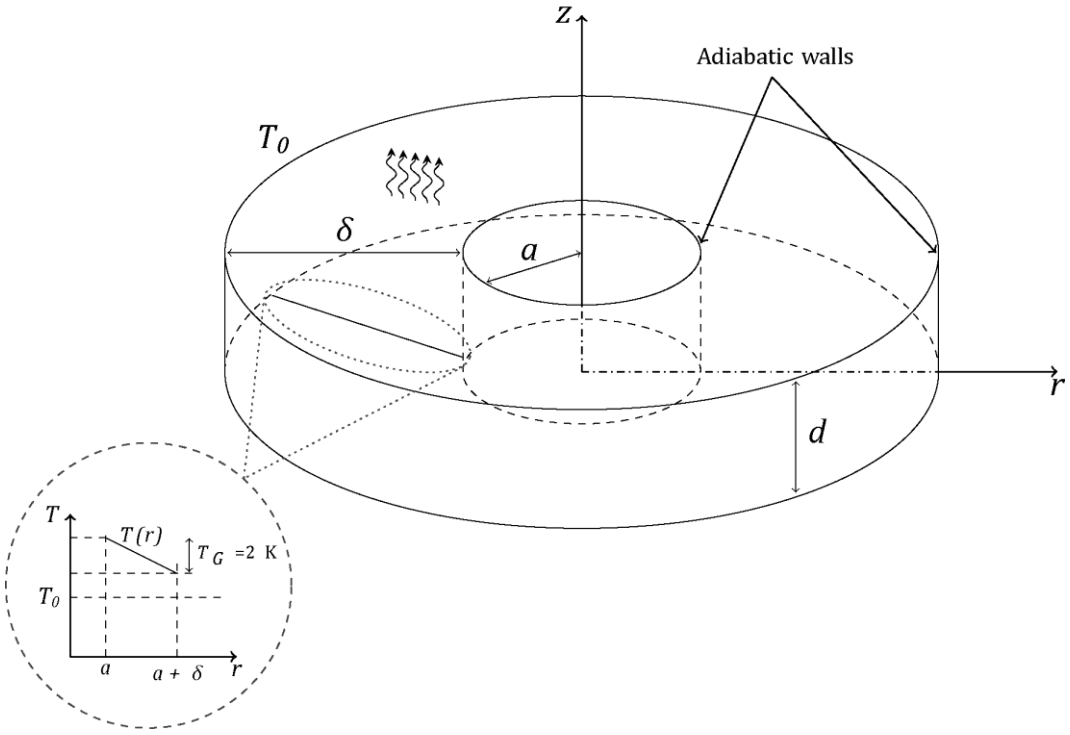

Figure 1. Lateral walls are considered adiabatic. The fluid is heated from below and the top surface is open to the atmosphere

The fluid layer behavior can be described by means of the momentum and mass balance equations and the energy conservation principle. These equations are non-dimensionalized using d as characteristic length, d^2/κ as characteristic time and ΔT as characteristic temperature difference, as previously done in [10]. The equations become respectively:

$$\nabla \cdot \boldsymbol{u} = 0, \tag{1}$$

$$\partial_t \mathbf{u} + (\mathbf{u} \cdot \nabla)\mathbf{u} = \mathrm{Pr} \cdot \left(-\nabla p + \nabla^2 \mathbf{u} + \mathrm{Ra}\Theta \mathbf{e}_z \right), \tag{2}$$

$$\partial_t \Theta + \boldsymbol{u} \cdot \nabla \Theta = \nabla^2 \Theta. \tag{3}$$

In the equations governing the system $\boldsymbol{u}$ is the velocity field with the three components expressed in cylindrical coordinates r, φ and z, i.e., u_r, u_φ and u_z. Θ is the flow temperature, and p is the pressure. In these equations the operators are expressed in cylindrical coordinates and $\boldsymbol{e}_z$ is the unit vector in the z direction. The Boussinesq approximation is used for turbulence modeling as it is usual in this sort of problems [25]. Boundary conditions are similar to those of references [10, 17]. Non-slip wall condition (velocity equal to zero) is imposed on the lateral walls and on the bottom plate. A linearly varying temperature distribution is imposed on the bottom plate, while lateral walls are

considered as adiabatic. On the top surface, the thermo-capillarity forces are modeled through the Marangoni condition [10], whereas the heat transfer to the atmosphere is simulated by the Biot condition. Notice that the dimensionless numbers presented in the introduction (Sec.1) appear in eqs. (1)-(3) and in the boundary conditions summarized in Table 1.

Table 1: Boundary conditions

$z = 0$	$z = d$	$r = a, a+\delta$
$u_r = 0$	$\partial_z u_r + \mathrm{Ma}\partial_r \Theta = 0$	$u_r = 0$
$u_\phi = 0$	$r\partial_z u_\phi + \mathrm{Ma}\partial_\phi \Theta = 0$	$u_\phi = 0$
$u_z = 0$	$u_z = 0$	$u_z = 0$
$\Theta = \Delta T - (T_G/\delta) r$	$\partial_z \Theta + \mathrm{Bi}\cdot\Theta = 0$	$\partial_n \Theta = 0$

Numerical Method

The temperature gradient on the bottom surface induces motion on the flow until a steady state, commonly know as basic state, is reached. Since the flow is laminar and due to the domain's symmetries, the basic state will be obtained under the assumption of 2D axisymmetric solution, and thus the dependency with ϕ can be neglected. Eqs. (1)-(3) developed for the cylindrical case then become:

$$r^{-1}\partial_r(ru_r) + \partial_z u_z = 0, \tag{4}$$

$$\mathrm{Pr}^{-1}(u_r\partial_r u_r + u_z\partial_z u_r) = -\partial_r p + \Delta_c u_r - \frac{u_r}{r^2}, \tag{5}$$

$$\mathrm{Pr}^{-1}(u_r\partial_r u_z + u_z\partial_z u_z) = -\partial_z p + \Delta_c u_z + \mathrm{Ra}\Theta, \tag{6}$$

$$u_r\partial_r\Theta + u_z\partial_z\Theta = \Delta_c\Theta, \tag{7}$$

where $\Delta_c = r^{-1}\partial_r(r\partial_r) + \partial_z^2$ is the Laplacian operator in cylindrical coordinates, simplified according to the previously mentioned symmetries.

The previous system of equations (4-7) can be solved in different ways, being spectral methods the most widely used [26]. Among the different spectral methods, the collocation method [27] is chosen in this work due to its accuracy and simplicity. The procedure is started by expanding the fluid variables in a truncated series of orthonormal Chebyshev polynomials, as

$$X^i(r,z) \approx \sum_{n=0}^{N}\sum_{m=0}^{M} a_{nm}^i \Im_n(r)\Im_m(z) \tag{8}$$

where $i = 1,\ldots,4$ and X^i stands for the four different flow variables, i.e., p, u_r, u_z, and Θ, respectively. $\Im_j(x)$ is the Chebyshev polynomial of the first kind of degree j. The polynomial coefficients, a_{nm}^i, are now the unknowns of the problem with the superscript indicating the corresponding flow variables. The flow variables expanded expressions from eq.(8) are substituted into eqs. (1), (2) and (3) and in the boundary conditions (Table 1). The

collocation method continues by evaluating the resultant equations in the Chebyshev-Gauss-Lobatto (CGL) points [28]. CGL points are defined as:

$$r_i = cos\left(\pi \frac{i}{N}\right),\ i = 0,1,\ldots,N,$$

$$z_i = cos\left(\pi \frac{i}{M}\right),\ i = 0,1,\ldots,M$$

where N and M correspond to the order of the method in radial and axial direction, respectively. The use of CGL points is especially of interest when dealing with boundary effects [26] since the collocation points tend to concentrate near the boundaries. A specially developed procedure proposed by Mancho et al. [5], consisting on projecting the equations by the normal to the boundaries, is used to impose the boundary condition for the pressure. This procedure avoids the problem of the spurious modes as stated by Bernardi and Maday [29]. The pressure is determined with respect to an additive constant.

The non-linearity of the problem is solved by using a Newton-like iterative method, taking as first approach either the solution of the linearized problem (neglecting the nonlinear part of eq. (5) and eq. (6)) or a previously known basic state "nearby" the new one. Convergence is typically obtained in less than 20 iterations as shown in the convergence test performed by Hoyas et al. [10].

The basic state is stable for low Ra. As Ra is increased (and thus the Ma for a given Bo), the basic state becomes unstable and several bifurcations arise. The purpose of this analysis is to determine the critical Ra and Ma values and the shape of growing instabilities for fixed Biot, Prandtl and Bond numbers.

The flow stability is analyzed by perturbing the solution for the basic state with perturbation fields depending on the three cylindrical coordinates, *r*, φ and *z*. Applying again the axial symmetry of the problem, and thus periodicity along the azimuthal direction, φ, fluid magnitudes may be expanded in Fourier modes over φ as:

$$X(r,\varphi,z,t) = X_b(r,z) + X_p(r,z)e^{ik\varphi+\lambda t} \tag{9}$$

where subscripts *b* and *p* stand for the basic state and the induced perturbation, respectively; and $k \geq 0$ is the wave number. It is important to remark again that the basic state does not depend on φ.

The real part of the eigenvalue, λ, characterizes the stability. For $Re(\lambda) < 0$ the solution is stable since the perturbation tends to dissipate. For $Re(\lambda) \geq 0$ the solution is unstable. In this latter case, the bifurcation might be stationary (imaginary part of λ equal to zero) or oscillatory (when the imaginary part of λ is non-zero).

Once the Fourier modes of the flow variables (eq.(9)) are substituted into the general equations (1-3) and the BCs from Table 1, the problem is linearized as shown by [17]. The system then becomes:

$$[A]\overline{X} = \lambda[B]\overline{X} \tag{10}$$

Due to the boundary conditions the matrix [*B*] is singular and thus not all the eigenvalues have a finite value. This issue is solved by using a transformation technique, developed by Navarro et al. [30], specifically designed for thermo-convective problems. The largest eigenvalue obtained through this transformation corresponds to the largest finite

eigenvalue of the original problem. The computational code was validated experimentally in [15] and the generalization of the code to Pr < 50 was validated in [17], using the same procedure as in [10].

Results and discussion

The analysis intends to determine the critical Rayleigh number (Ra_c) and critical Marangoni number (Ma_c) for different conditions depending on the Biot, Prandtl and Bond numbers and on the domain aspect ratio, Γ. The critical condition is found when the real part of the eigenvalue of eq. (10) is equal to 0 and is associated to a critical wave number, *k*. Solving the eigenvalue problem also allows obtaining the eigenvectors of the solution that represents the shape of unstable modes.

Critical wave number

Figure 2 shows the critical wave number for each of the 6 combinations of Prandtl and Bond numbers analyzed in this work. The figure reports contour plots of the wave number for varying Γ, and Biot number. Two different colour scales are used: one for stationary modes going from light blue to yellow for increasing wave number and the other one for oscillatory modes going from light blue to dark blue for increasing wave number. Figure 2 shows the great variation of critical wave numbers and of the type of growing perturbation depending on the parameters object of the study. Moving along a constant Bi line for increasing Γ at low aspect ratios the modes are typically found to be steady then for a range of aspect ratios the modes are oscillatory and finally at higher aspect ratios the modes become again stationary. The wave number is found to increase with the aspect ratio suggesting that the characteristic wavelength of the disturbances is positively correlated with the domain depth. The precession of the modes along the domain for a limited range of Γ suggests that these aspect ratios should enable a better mixing and enhanced heat transfer performances.

Both increasing Pr and Bo, the Γ range which results in oscillatory solutions is reduced while the characteristic wavelength is slightly affected. The Prandtl number effect can be explained with the increase of damping due to viscous forces, while the Bo effect is related to the decrease of thermocapilarity forces at a given Ra. Increasing the Bi for all the other parameters fixed, results in a small decrease of the wave number and in the possible suppression of oscillations due to the decrease of the vertical temperature gradient through the domain.

Evolution of the critical Rayleigh number

Figure 3 reports the values of the critical Rayleigh number versus the domain aspect ratio Γ at Bi equal to 0.8 for three different cases. Going through Figure 3 from top to bottom, the cases are: Pr = 1, Bo = 5 (corresponding to the case shown in Fig. 2(e)), Pr = 1, Bo = 50 (Fig. 2(f)), and Pr = 50, Bo = 50 (Fig. 2(b)). It is worth to remark that the value of the wave number along the curve is not continuous. Hollow circles stand for stationary bifurcations, whereas bold ones indicate oscillatory ones.

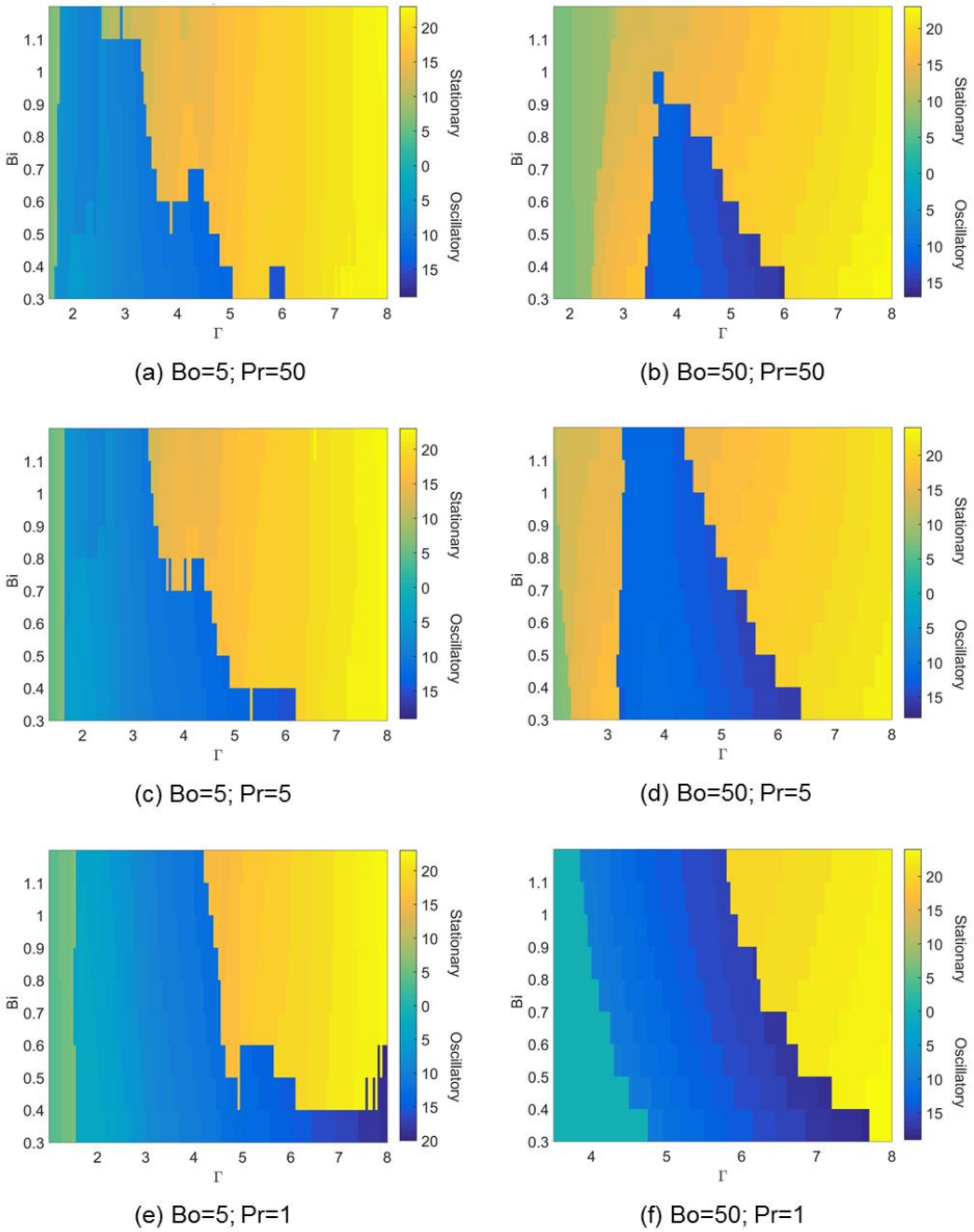

Figure 2: Critical wave number for the different numerical experiments analyzed in this work, the results are divided in stationary (Imag(λ)=0) and oscilaroty cases (Imag(λ)≠0). Left column cases with Bo= 5 and for decreasing values of the Prandtl number. Right column cases with Bo = 50

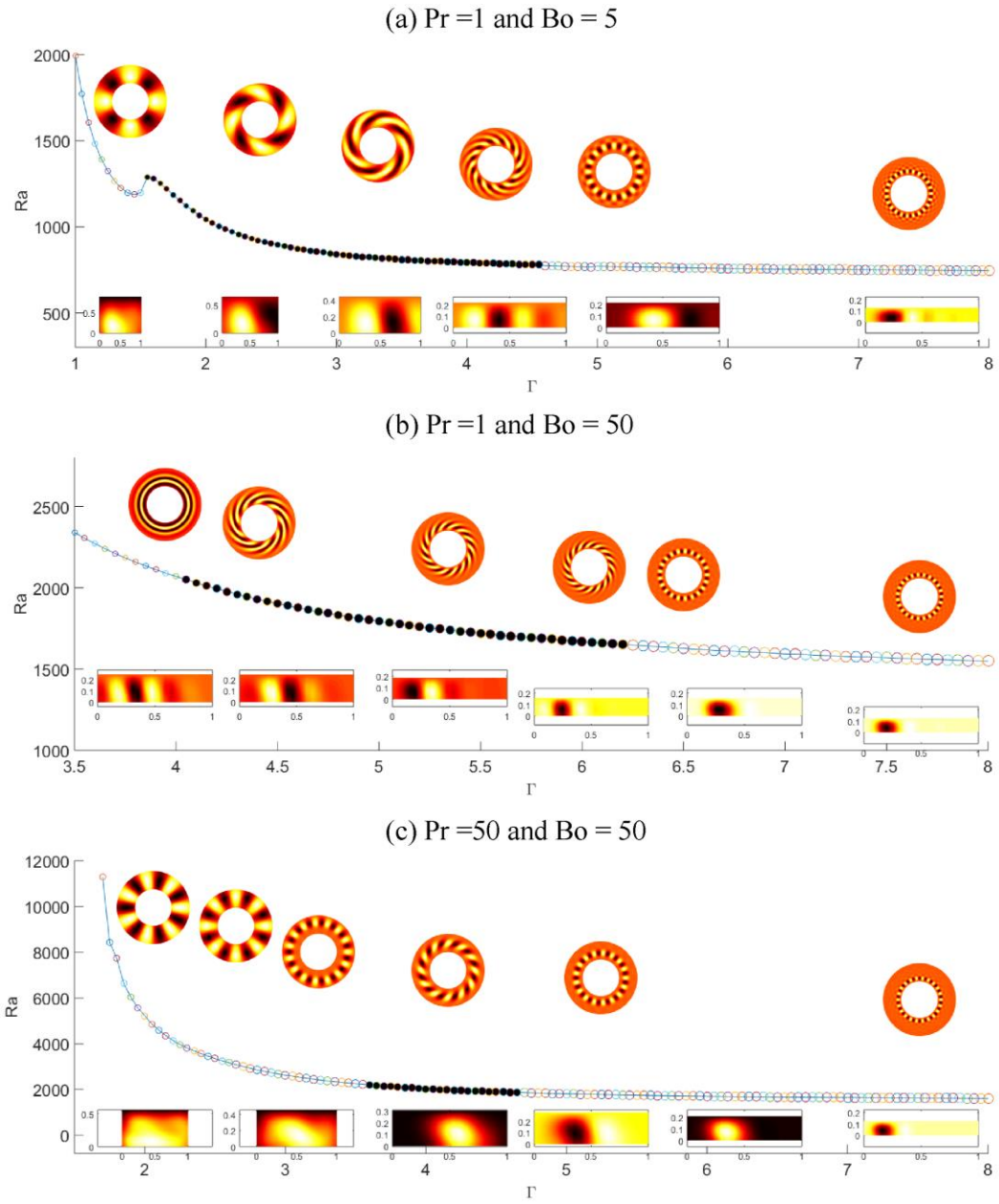

Figure 3: Evolution of the critical Ra with Γ for Bi = 0.8, and (a) Pr = 1 and Bo = 5, (b) Pr = 1 and Bo = 50, (c) Pr = 50 and Bo = 50. Empty circles stand for stationary bifurcations, whereas bold ones indicate oscillatory ones. The size of the circle indicates the wave number in a scale from *k*=0 (the smallest circle) to *k*=24 (the largest one)

Additionally, the size of the marker is related with the value of the wave number, the smallest circle represents a value of k=0 and the largest one a value of k=24. The wave number increases with the aspect ratio of the domain, Γ (as also shown in Figure 1), while the critical Rayleigh number decreases. This same tendency was previously found by the authors in [22]. Figure 3 also includes representative top r-φ plane isotherms plotted above the curves. The temperature field is non-dimensionalized with respect to the maximum Θ. Below the line the corresponding z-r planes are also reported. Several types of instabilities are found along the constant Bi curves. As an example in Fig. 3(b), for low aspect ratios, $\Gamma = 3-4$, Stationary rolls (SR) are found; passing through a region of oscillatory Hydrothermal Wave of the first kind (HWI), $\Gamma = 4-6.2$; and finally, for large aspect ratios, $\Gamma = 6.2-8$ Longitudinal Rolls (LR) appear as a result of the temperature gradient along the bottom wall which provides a stronger effect in the inner part of the domain.

Figure 3(a) reports in the same fashion as in Figure 3(b) the information for the case of Pr = 1 and Bo = 5 (Fig. 2(c)). For small aspect ratios a flower-like perturbation (as the ones obtained in [22]) appears instead of the stationary rolls of the former case. Following the curve, the arising perturbations are the same, passing through a region of oscillatory Hydrothermal Wave of the first kind (HWI), and finally for large aspect ratios, Longitudinal Rolls. It has to be remarked from comparison of Fig. 3(a) and Fig. 3(b) that the critical wave number in the regions of HWI and LR is smaller in the former case. This means that the critical wave number is increased when the Marangoni number decreases, while the critical Rayleigh number follows the opposite tendency.

Comparing the curves from Fig. 3(b) and Fig. 3(c) the effect of the Prandtl number can be assessed. The increase of the Prandtl number has a remarkable effect on the substantial increase of the critical Rayleigh number at which the modes become unstable due to the increase of viscous effects. The aspect ratio at which the different regimes appear is modified for $\mathrm{Pr} > 1$; in fact the region of HWI is delayed (in aspect ratio) and becomes narrower, being the transition to LR also anticipated. Moreover, the viscous effect are found to be responsible of the arising of a flower-like perturbation for low aspect ratios.

Co-dimension two points

As Fig. 2 and Fig. 3 illustrate, different kind of competing solutions appear on localized regions of the Γ-Bi plane. The boundaries of these zones are made up of co-dimension two points, where two of the competing solutions may appear at the same time. The evolution of the critical Marangoni number and of the Biot number of all the co-dimension two points found in the present work is shown in Fig. 4. Notice that all these points are obtained for different values of the aspect ratio Γ.

The main result shown in the figure is that most of the co-dimension two points have little dependence on the Prandtl number since the points seem to lay along two curves of equal Bond number: one for Bo = 5 and the other for Bo = 50. Of course at higher Bond number the critical Marangoni number is lower and practically constant since the instabilities are mostly triggered by the buoyancy effects and a slight increase of the critical Marangoni number is required to compensate the instabilizing effect of the decrease of the Biot number.

Some outliers with respect to the Ma-Bi curves are found among the low Bond cases for domains with high aspect ratio, where the Biot number is the dominant parameter as seen in previous works as [22]. On the other hand for high Bond numbers (Bo = 50), the flow is dominated by the thermoconvective phenomena, and Biot number is not representative there.

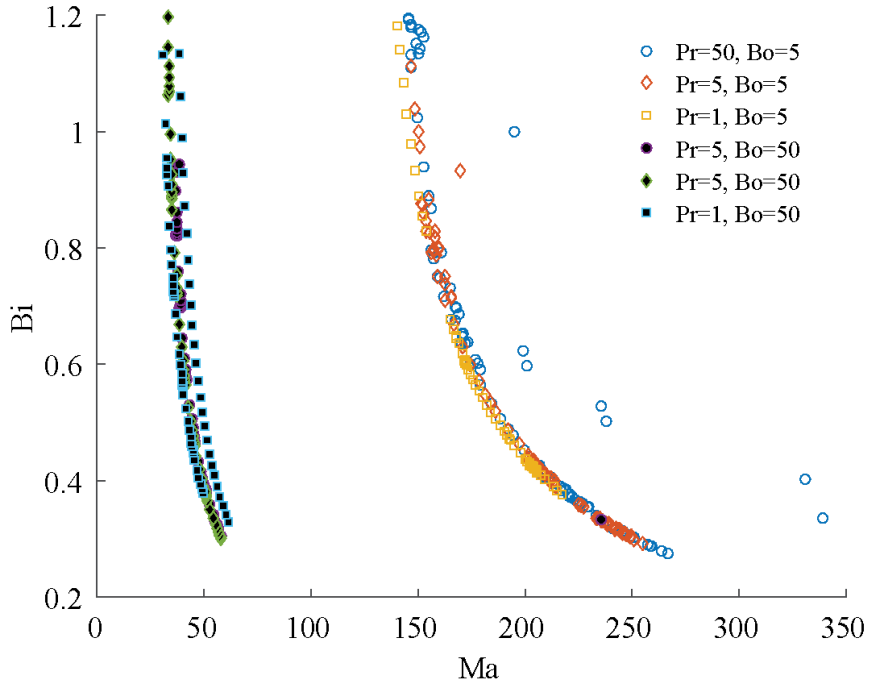

Figure 4: Representation of the critical Marangoni number and Biot number of all the codimension two points found in the present analysis

Conclusions

This paper assesses the influence of the gravitational and capillarity forces of the onset of flow instabilities in a Bérnard-Marangoni convection problem. Numerical simulations have been conducted in an annular domain with a temperature gradient imposed at its lower wall. This gradient induces a velocity field in the flow, that evolves until a basic state is reached. The analysis is performed for 3 different values of the Prandtl numbers, ranging from a viscosity dominated problem (Pr=50) to problems in which the nonlinear flow effects are important (Pr=1), and addressing an intermediate problem representative of the conditions of water at ambient conditions (Pr=5). This work also addresses the influence of the surface tension and the thermocapillarity in perturbing the computed instabilities by analyzing two different ranges of the Bond numbers (5 and 50).

The critical wave number for each combination of Biot number on the free surface and domain aspect ratio has been studied. The perturbations are divided in stationary and oscillatory depending on the imaginary part of the eigenvalue. The increase of Γ allows to pass from a stationary unstable mode to an oscillatory one, then further increasing Γ to

stationary again. The wave number is found to be positively correlated with the domain aspect ratio.

It has been showed that different perturbation types share a common boundary in the Bi- Γ plane, these points where two competing solutions are found are known as co-dimension two points.

For a constant value of the Biot number (Bi=0.8), the critical Rayleigh number generally decreases with the domain aspect ratio, while the critical wave number tends to increase. Different instabilities are found along the constant Bi line, mixing both oscillatory and stationary ones. The increase of Pr has a stabilizing effect on the flow which becomes unstable for higher Rayleigh numbers; as well the increase of Bo has an unstabilizing effect, resulting in higher wave numbers. The range of aspect ratios which interested by oscillatory solutions also increases with increasing Bo. For low Prandtl number, the type of the arising instabilities are different in the cases of Bo=5 and Bo=50 , in particular for low aspect ratios, Γ between 3 and 4 where higher bond number promotes the appearance of Stationary Rolls.

The co-dimension two points present a tendency that does not depend on the Prandtl number since most of the points lay along two curves (one for each value of the Bond number considered during this work) in the Biot-Marangoni plane. It is shown that for high Bond number (Bo = 50), the thermocaliparity effects are negligible and the Biot number plays a small role in the flow description. On the other hand for smaller Bond numbers (Bo = 5) some points lay out the the curve. These cases are related with a high aspect ratio of the flow domain.

Acknowledgments

The authors would like to thank Mr. Salvador Hoyas for fruitful conversations about the paper. This work was supported by a generous grant of computer time from the supercomputing center of the UPV. This work has been partially supported by the Spanish R&D National Plan, grant number ESP2013-41052-P.

References

[1] Bénard, H., Les tourbillons cellulaires dans une nappe liquid, *Rev. Gen. Sci. Pure Appl.*, 11 (1900), pp. 1261-1271.
[2] Zhang, W., Zhou, J., Optimal control of a viscous shallow water equation, *Advances in Mathematical Physics*, vol 2013 (2013), 715959.
[3] Es Sakhy, R., El Omari, K., Le Guer, Y., Blancher, S, Rayleigh–Bénard–Marangoni convection in an open cylindrical container heated by a non-uniform flux, *International Journal of Thermal Sciences*, 86 (2014), pp. 198-209.
[4] Mercier, J. F., Normand, C, Buoyant-thermocapillary instabilities of differentially heated liquid layers, *Physics of Fluids (1994-present)*, 8 (1996), 6, pp. 1433-1445.
[5] Mancho, A. M., Herrero, H., Burguete, J, Primary instabilities in convective cells due to nonuniform heating, *Physical Review E*, 56 (1997), 3, pp. 2916-2923.
[6] Herrero, H., Mancho, A. M, Influence of aspect ratio in convection due to nonuniform heating. *Physical Review E*, 57 (1998), 6, pp. 7336-7339.
[7] Ezersky, A. B., Garcimartin, A., Burguete, J., Mancini, H. L., Pérez-García, C, Hydrothermal waves in Marangoni convection in a cylindrical container, *Physical Review E*, 47 (1993),2, pp. 1126-1131.
[8] Bammou, L., Blancher, S., Le Guer, Y., El Omari, K., Benhamou, B., Linear stability analysis of Poiseuille–Bénard–Marangoni flow in a horizontal infinite liquid film, *International Communications in Heat and Mass Transfer*, 54 (2014), pp. 126-131.

[9] Pardo, R., Herrero, H., Hoyas, S., Theoretical study of a Bénard–Marangoni problem. *Journal of Mathematical Analysis and Applications*, 376 (2011), 1, pp. 231-246.
[10] Hoyas, S., Herrero, H., Mancho, A. M, Thermal convection in a cylindrical annulus heated laterally. *Journal of Physics A: Mathematical and General*, 35 (2002), 18, pp. 4067-4083.
[11] Hoyas, S., Herrero, H., Mancho, A. M., Bifurcation diversity of dynamic thermocapillary liquid layers, *Physical Review E*, 66 (2002), 5, 057301.
[12] Peng, L., Li, Y. R., Shi, W. Y., Imaishi, N, Three-dimensional thermocapillary–buoyancy flow of silicone oil in a differentially heated annular pool, *International Journal of Heat and Mass Transfer*, 50 (2007), 5, pp. 872-880.
[13] Shi, W., Liu, X., Li, G., Li, Y. R., Peng, L., Ermakov, M. K., Imaishi, N., Thermocapillary convection instability in shallow annular pools by linear stability analysis, *Journal of Superconductivity and Novel Magnetism*, 23 (2010), 6, pp. 1185-1188.
[14] Wertgeim, I. I., Kumachkov, M. A., Mikishev, A. B., Periodically excited Marangoni convection in a locally heated liquid layer, *The European Physical Journal Special Topics*, 219 (2013), 1, pp. 155-165.
[15] Hoyas, S., Mancho, A. M., Herrero, H., Garnier, N., Chiffaudel, A., Bénard–Marangoni convection in a differentially heated cylindrical cavity, *Physics of Fluids (1994-present)*, 17 (2005), 5, 054104.
[16] Garnier, N., Chiffaudel, A., Two dimensional hydrothermal waves in an extended cylindrical vessel, *The European Physical Journal B-Condensed Matter and Complex Systems*, 19 (2001), 1, pp. 87-95.
[17] Torregrosa, A. J., Hoyas, S., Pérez-Quiles, M. J., Mompó-Laborda, J. M., Bifurcation diversity in an annular pool heated from below: Prandtl and biot numbers effects, *Communications in Computational Physics*, 13 (2013), 2, pp. 428-441.
[18] Hoyas, S., Gil, A., Fajardo, P., Pérez-Quiles, M. J.. Codimension-three bifurcations in a Bénard-Marangoni problem, *Physical Review E*, 88 (2013), 1, 015001.
[19] Eckert, E. R. G., Goldstein, R. J., Ibele, W. E., Patankar, S. V., Simon, T. W., Kuehn, T. H., Strykowski, P.J., Tamma, K.K., Bar-Cohen, A., Heberlein, J.V.R., Davidson, J.H., Bischof, J., Kulacki, F.A., Kortshagen, U., Garrick, S., Heat transfer—a review of 1997 literature, *International Journal of Heat and Mass Transfer*, 43 (2000), 14, pp. 2431-2528.
[20] O'Shaughnessy, S. M., Robinson, A. J., Heat transfer near an isolated hemispherical gas bubble: The combined influence of thermocapillarity and buoyancy, *International Journal of Heat and Mass Transfer*, 62 (2013), pp. 422-434.
[21] Hoyas, S., Fajardo, P., Gil, A., Perez-Quiles, M. J., Analysis of bifurcations in a Bénard–Marangoni problem: Gravitational effects, *International Journal of Heat and Mass Transfer*, 73 (2014), pp. 33-41.
[22] Hoyas, S., Fajardo, P., Pérez-Quiles, M. J., Influence of geometrical parameters on the linear stability of a Bénard-Marangoni problema, *Physical Review E*, 93 (2016), 4, 043105.
[23] Smith, M. K., Davis, S. H., Instabilities of dynamic thermocapillary liquid layers. Part 1. Convective instabilities, *Journal of Fluid Mechanics*, 132 (1983), pp. 119-144.
[24] Favre, E., Blumenfeld, L., Daviaud, F., Instabilities of a liquid layer locally heated on its free surface, *Physics of Fluids (1994-present)*, 9 (1997), 5, pp. 1473-1475.
[25] Chandrasekhar, S., *Hydrodynamic and Hydromagnetic Stability*. International Series of Monographs on Physics, Oxford-Clarendon Press, 1961.
[26] Jimenez, J., Hoyas, S., Turbulent fluctuations above the buffer layer of wall-bounded flows, *Journal of Fluid Mechanics*, 611 (2008), pp. 215-236.
[27] Orszag, S. A. Comparison of pseudospectral and spectral approximation. *Studies in Applied Mathematics*, 51 (1972), 3, pp. 253-259.
[28] Canuto, C., Hussaini, M. Y., Quarteroni, A., Zang, T. A., *Spectral methods in Fluid Dynamics*, Springer-Verlag, 1988.
[29] Bernardi, C., Maday, Y, *Approximations spectrales des problemes aux limites elliptiques*. Springer-Verlag, 1992.
[30] Navarro, M. C., Herrero, H., Hoyas, S., Chebyshev collocation for optimal control in a thermoconvective flow, *Comm. Comput. Phys*, 5 (2009), 2-4, pp. 649-666.

Paper submitted: June 28, 2016
Paper revised: September 6, 2016
Paper accepted: September 6, 2016